Cell, Vol. 109, 371–381, May 3, 2002, Copyright ©2002 by Cell Press

Prickle Mediates Feedback Amplification to Generate Asymmetric Planar Cell Polarity Signaling

David R.P. Tree,[1,2] Joshua M. Shulman,[3] Raphaël Rousset,[4,6] Matthew P. Scott,[4] David Gubb,[2] and Jeffrey D. Axelrod[1,5]

[1]Department of Pathology
Stanford University School of Medicine
300 Pasteur Drive
Stanford, California 94305

[2]Department of Genetics
University of Cambridge
Downing Street
Cambridge, CB2 3EH
United Kingdom

[3]Department of Pathology
Brigham and Women's Hospital and Harvard Medical School
221 Longwood Avenue
Boston, Massachusetts 02115

[4]Departments of Developmental Biology and Genetics
Howard Hughes Medical Institute
Beckman Center B300
Stanford University School of Medicine
Stanford, California 94305

Summary

Planar cell polarity signaling in *Drosophila* requires the receptor Frizzled and the cytoplasmic proteins Dishevelled and Prickle. From initial, symmetric subcellular distributions in pupal wing cells, Frizzled and Dishevelled become highly enriched at the distal portion of the cell cortex. We describe a Prickle-dependent intercellular feedback loop that generates asymmetric Frizzled and Dishevelled localization. In the absence of Prickle, Frizzled and Dishevelled remain symmetrically distributed. Prickle localizes to the proximal side of pupal wing cells and binds the Dishevelled DEP domain, inhibiting Dishevelled membrane localization and antagonizing Frizzled accumulation. This activity is linked to Frizzled activity on the adjacent cell surface. Prickle therefore functions in a feedback loop that amplifies differences between Frizzled levels on adjacent cell surfaces.

Introduction

Both neutrophils and aggregating *Dictyostelium* cells respond to extrinsic gradients of chemoattractants by polarizing their cytoskeletons and migrating toward the source of the signal (Parent et al., 1998; Servant et al., 2000). Remarkably, the slope of the gradient can be quite small—only ~1%–2% across a cell diameter—yet these cells respond by producing highly localized concentrations of signaling molecules and cytoskeletal reorganizing activity. Such dramatic responses to shallow signal gradients result from feedback mechanisms that amplify initial small differences (Servant et al., 2000). A similar cytoskeletal reorganization occurs during the response of epithelial cells to extrinsic polarizing signals (Wong and Adler, 1993) and also involves a feedback mechanism (Axelrod, 2001; Strutt, 2001).

Drosophila melanogaster epithelial cells acquire a polarity orthogonal to their apical-basal axes, referred to as planar cell polarity (PCP; Adler, 1992; Gubb, 1993; Eaton, 1997; Shulman et al., 1998). PCP is manifested in the parallel orientation of hairs and bristles on the adult body and appendages and in the regular patterns of ommatidial orientation in the eye. Polarization of these structures is controlled by the PCP genes, mutants of which produce stereotypical, nonparallel polarity patterns. The PCP genes include a core group that affects polarity over the whole body, as well as additional, tissue-specific components that are regulated by the core group (Adler, 1992; Shulman et al., 1998).

The core group of genes includes *frizzled (fz)*, *dishevelled (dsh)*, *prickle-spiny-legs (pk)*, and *flamingo (fmi)*. Fz is a transmembrane receptor (Vinson et al., 1989) that, in addition to its role in PCP, acts redundantly with its homolog, Fz2, as a receptor for Wingless (Wg; Bhanot et al., 1996, 1999; Bhat, 1998; Chen and Struhl, 1999). Because Fz proteins function as Wnt receptors, it is possible that one or more *Drosophila* Wnts function as PCP ligands, although there is currently no direct evidence for this. Dsh is a cytoplasmic protein required for transduction of both Wg and PCP signals (Klingensmith et al., 1994; Thiesen et al., 1994). One of three highly conserved domains in Dsh, the DEP domain, mediates interaction of Dsh with the cell cortex and is required for PCP but not Wg signaling (Axelrod et al., 1998, 2001). Flamingo (Fmi; Usui et al., 1999; also known as Starry night; Chae et al., 1999) is a seven pass transmembrane cadherin superfamily member, and Prickle-spiny-legs (Pk) is a novel protein containing three LIM domains and a conserved "PET" domain (for Prickle, Espinas, and Testin; Gubb et al., 1999). Analysis of overexpression phenotypes suggests that information in the PCP signaling pathway flows from the receptor Fz to the cytoplasmic protein Dsh, which in turn acts upon the tissue-specific genes (Krasnow et al., 1995). The relationships of Pk and Fmi to this putative signaling pathway remain unclear.

The Pk locus produces three alternately spliced transcripts (pk^{pk}, pk^{M}, and pk^{sple}) that encode isoforms that differ in their N-terminal regions (Gubb et al., 1999). While loss of individual Pk isoforms produces tissue-specific effects, the loss of all Pk isoforms ($pk^{pk\text{-}sple}$ alleles) leads to PCP phenotypes throughout the adult fly. Alleles of the $pk^{pk\text{-}sple}$ class produce wing hair phenotypes similar to those displayed by *fz* and *dsh*, implying that Pk is required for Fz/Dsh-mediated PCP signaling. However, epistasis tests using loss-of-function *pk* alleles have not allowed its placement in a linear signaling cas-

[5]Correspondence: jaxelrod@cmgm.stanford.edu

[6]Present address: Institut de Recherches "Signalisation, Biologie du Développement et Cancer," Centre de Biochimie, UMR 6543 CNRS, Universite de Nice, Parc Valrose, 06108 Nice Cedex 2, France.

cade with Fz and Dsh (Gubb and Garcia-Bellido, 1982; Krasnow et al., 1995; Gubb et al., 1999). These kinds of epistasis data are sometimes indicative of parallel or feedback pathways.

Numerous models have been proposed for the extracellular cue that provides orientation during PCP signaling. These include gradients of signaling molecules, sequential relay of cell to cell signals, and tesselation (Adler, 1992; Eaton, 1997; Gubb, 1998; Shulman et al., 1998; Reifegerste and Moses, 1999; Strutt and Strutt, 1999). While recent work provides evidence that gradients influence the activity of the PCP pathway (Yang et al., 2002), prior evidence is consistent with a role for any of these or other mechanisms, either singly or in combination.

In pupal wings, both the Fz and Dsh proteins become localized to the distal side of the cell (Axelrod, 2001; Strutt, 2001), and the protocadherin Fmi localizes to proximal-distal (P-D) intercellular boundaries, most likely on both sides of the boundary (Usui et al., 1999). At the beginning of the pupal period, Dsh is recruited from the cytoplasm to the cell cortex in response to Fz/PCP signaling (Axelrod, 2001). Initially, Dsh forms an apparently symmetric apical ring around the boundary of each cell. However, by 18–24 hr after puparium formation (APF), Dsh becomes preferentially localized to the distal surfaces of the hexagonally shaped cells. This distal distribution is most apparent by 30 hr APF. Fz relocalizes to the distal surfaces in a similar fashion (Strutt, 2001; our unpublished observations). The pattern of Dsh localization is both dependent on Fz and required to generate PCP. The discrete localization of Fz and Dsh appear to result from a feedback amplification mechanism, since activity of the transducer, Dsh, is required to generate asymmetric localization of both Fz and Dsh (Axelrod, 2001; Strutt, 2001). The mechanism for this feedback is unknown.

Here, we demonstrate that Pk is required to generate asymmetry of Fz/Dsh activity. We show that Pk localizes to the proximal side of pupal wing cells, where it antagonizes Fz and Dsh localization by binding the Dsh DEP domain and preventing Dsh cortical localization. This activity is linked to Fz/Dsh activity on the adjacent cell surface. Beginning from a nearly symmetrical distribution of Fz and Dsh, the system acts as a feedback loop that amplifies small differences in initial Fz activity on adjacent P-D intercellular boundaries, resulting in large differences between proximal and distal Fz, Dsh, and Pk.

Results

Loss of Pk Function Abolishes the Acquisition of Asymmetry during Fz Activation

PCP signaling occurs during the 30 hr beginning at the start of the pupal period and ending just before the initiation of prehair development (Krasnow and Adler, 1994; Adler et al., 1994a, 1994b; Axelrod, 2001). Dsh localization is dependent on the dynamic pattern of Fz activation and localization (Axelrod, 2001; Strutt, 2001). At the beginning of the pupal period, cytoplasmic Dsh is recruited roughly symmetrically to the apical membrane (Figure 1A; Axelrod, 2001). Between 18 and 24 hr APF, Dsh localization becomes biased toward the distal side of cells, and by 30 hr APF most of the cortical Dsh is found at the distal boundaries of the hexagonal wing cells, where Fz is also localized at this time (Figure 1B; Axelrod, 2001; Strutt, 2001). Both Fz and Dsh proteins must be functional in order to observe any asymmetry.

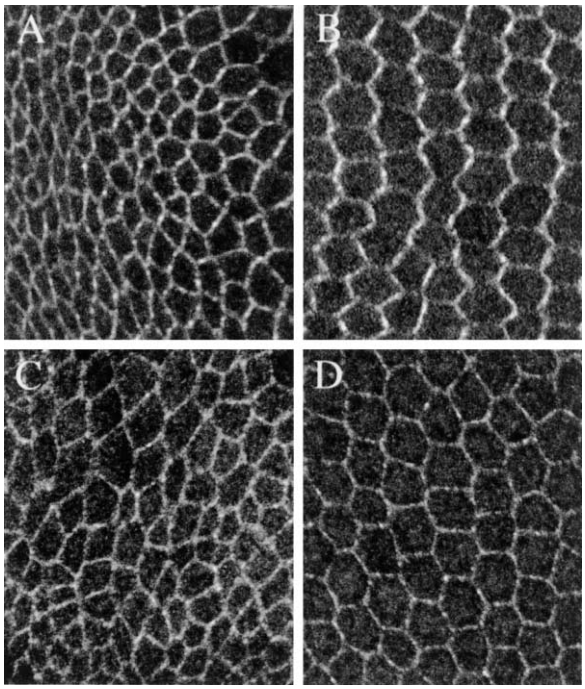

Figure 1. Localization of Dsh in Wild-Type and *pk* Mutant Wings

Confocal images of pupal wings. For all images, proximal is to the left and anterior is up.

(A and B) In wild-type pupal wings, Dsh::GFP at 2.5 hr APF is localized symmetrically around the apical cell surface (A). By 30 hr APF, Dsh::GFP is strongly localized to the distal boundary of each cell and correlates to the site of prehair localization (B).

(C and D) In a pupal wing lacking Pk, Dsh is found at the membrane at 2.5 hr APF (C) but remains symmetrically localized around the cell membrane at 30 hr APF (D).

To address the function of Pk, we examined the pattern of Dsh localization in *pk* mutants. In a $pk^{pk\text{-}sple}$ mutant wing, Fz-dependent recruitment of Dsh to the membrane at the beginning of pupariation occurs as in wild-type (Figure 1C), implying that normal, nearly symmetric activation of Fz occurs. However, at later times, less Dsh accumulates at the cortex than in wild-type, and cortical Dsh fails to become asymmetrically localized, instead remaining symmetrically distributed even at 30 hr APF (Figure 1D). Similarly, Fz fails to localize asymmetrically in a $pk^{pk\text{-}sple}$ wing (Strutt, 2001). This implies that although PCP signaling is active, as assayed by the translocation of Dsh to the cortex, it fails to produce polarized Dsh and Fz localization. Therefore, Pk is not required for the initial activation of Fz signaling but is required to generate asymmetry during PCP signaling. Pk may thus be required in a feedback amplification mechanism.

Pk Localization and Activity at the Proximal Side of the Cell

To study the protein localization of Pk, we produced an antiserum to the Pk protein. In 2.5 hr APF pupal wings, staining with this antiserum demonstrates that Pk local-

izes circumferentially to the apical surface of wing cells (Figures 2A–2C). Much of the Pk protein is observed in an irregular pattern of foci that do not colocalize with Dsh. However, by 30 hr APF, Pk is found at P-D cell interfaces, producing a series of parallel zigzags that nearly colocalize with Dsh (Figures 2D–2F). Furthermore, by staining for Pk in wings containing $pk^{pk\text{-}sple}$ clones, it can be seen that Pk is present only on the proximal sides of cells (Figure 2G). Therefore, rather than being present on the distal side of the cell as are Dsh and Fz, Pk is found across the intercellular P-D interface, on the proximal side of the neighboring cell.

The presence of Pk at the proximal side of the cell suggests that Pk may be required for the distal accumulation of Dsh and Fz in the neighboring cell. We therefore asked whether Pk functions non-cell-autonomously. To do this, we examined Dsh localization in and around $pk^{pk\text{-}sple}$ loss-of-function clones. If Pk acts non-cell-autonomously, Dsh accumulation at the proximal clone border should resemble that in the interior of the clone, while Dsh accumulation at the distal clone border should be wild-type. These differences are somewhat subtle (compare Figures 1B and 1D) but can be detected and quantitated (Figures 2H and 2I). Within the clone, Dsh localization remains uniform around cells, as is seen in $pk^{pk\text{-}sple}$ mutant wings (Figure 2H). At the distal border of the clone, Dsh accumulates to levels similar to those achieved in the surrounding wild-type tissue (distal clone border mean pixel luminosity per boundary, 90.0 $\pm$ 9.5; compared with 92.1 $\pm$ 6.2 at surrounding wild-type P-D boundaries), indicating that Pk function at the proximal side of the wild-type cell promotes normal Dsh accumulation in the adjacent $pk^{pk\text{-}sple}$ mutant cell. In contrast, at the proximal border of the clone, Dsh is present at a lower level (mean pixel luminosity per boundary 76.2 $\pm$ 4.1) that is similar to the interior of the clone (mean pixel luminosity per boundary 78.8 $\pm$ 5.6), implying that Pk in the neighboring wild-type cell is unable to promote Dsh accumulation cell autonomously. Pk therefore functions at the proximal side of wing cells, where it promotes higher levels of Dsh accumulation at the distal cortical domain of the adjacent cell. This is consistent with the nonautonomous adult phenotype of $pk^{pk\text{-}sple}$ clones (Gubb et al., 1999).

Proximal Pk Localization Depends on Intercellular Differences in Fz Activity

To determine what controls proximal Pk localization, we examined Pk localization in various mutant backgrounds. In both *fz* and dsh^{1} mutant backgrounds, Pk remains associated with the membrane but fails to become asymmetrically distributed (Figures 3A and 3B) and colocalizes with Fmi, which is also symmetric in the mutants, as previously reported (Figures 3C and 3D; Usui et al., 1999). Asymmetric accumulation of Pk at the proximal cell surface therefore requires the activity of Fz and Dsh.

In the wild-type, Fz is present at high levels on the distal side of 30 hr APF pupal wing cells, while Pk is present only on the proximal sides of these cells, where Fz levels are low. We therefore asked if differences in Fz levels between adjacent cell surfaces result in Pk accumulation by studying the borders of *fz* mutant clones (Figures 3E–3G). Pk was seen to accumulate at

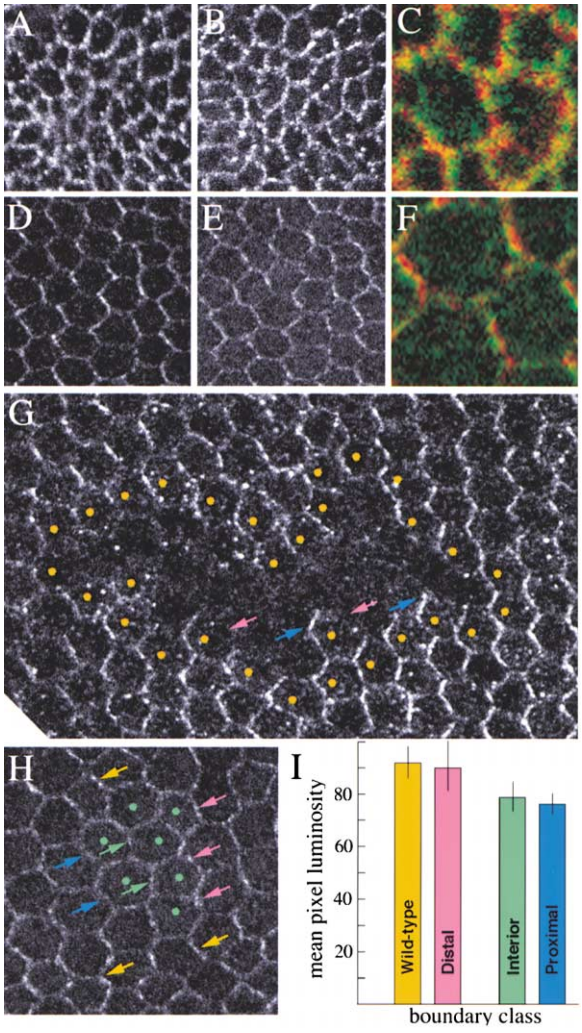

Figure 2. Pk Activity and Pk Protein Are Localized Proximally in Pupal Wing cells

Confocal images of pupal wings. Pk (A) and Dsh::GFP (B) are both symmetrically localized around the cell membrane in 2.5 hr APF pupal wing cells but do not precisely colocalize ([C], higher magnification merge of [A] and [B]; Pk is indicated in red and Dsh::GFP in green). By 30 hr APF, Pk (D) and Dsh::GFP (E) are found at the P-D boundaries of pupal wing cells.

(F) Higher magnification overlay of (D) and (E), with Pk indicated in red and Dsh::GFP in green.

(G) Pk staining of a 30 hr APF wing containing a $pk^{pk\text{-}sple13}$ mutant clone. Wild-type cells surrounding the clone are indicated by yellow dots. Pk protein is observed at the proximal (pink arrows) but not distal (blue arrows) boundaries of wild-type cells that abut mutant cells, revealing that Pk is localized to the proximal but not the distal boundaries of cells.

(H) Dsh::GFP in a $pk^{pk\text{-}sple13}$ clone at 30 hr APF. The mutant cells are indicated with green dots. Inside the clone, Dsh::GFP is present symmetrically at the membrane. At the distal edge of the clone, Dsh accumulates at a wild-type level (pink arrows; compare to wild-type boundaries, yellow arrows). At the proximal edge of the clone (blue arrows), Dsh::GFP accumulates at the same level as in the interior of the clone (green arrows).

(I) Mean pixel luminosities for boundaries between wild-type cells, between mutant cells (interior), and at the proximal and distal clone boundaries in (H) are shown in graphical form, with standard deviations. Numerical values are given in the text.

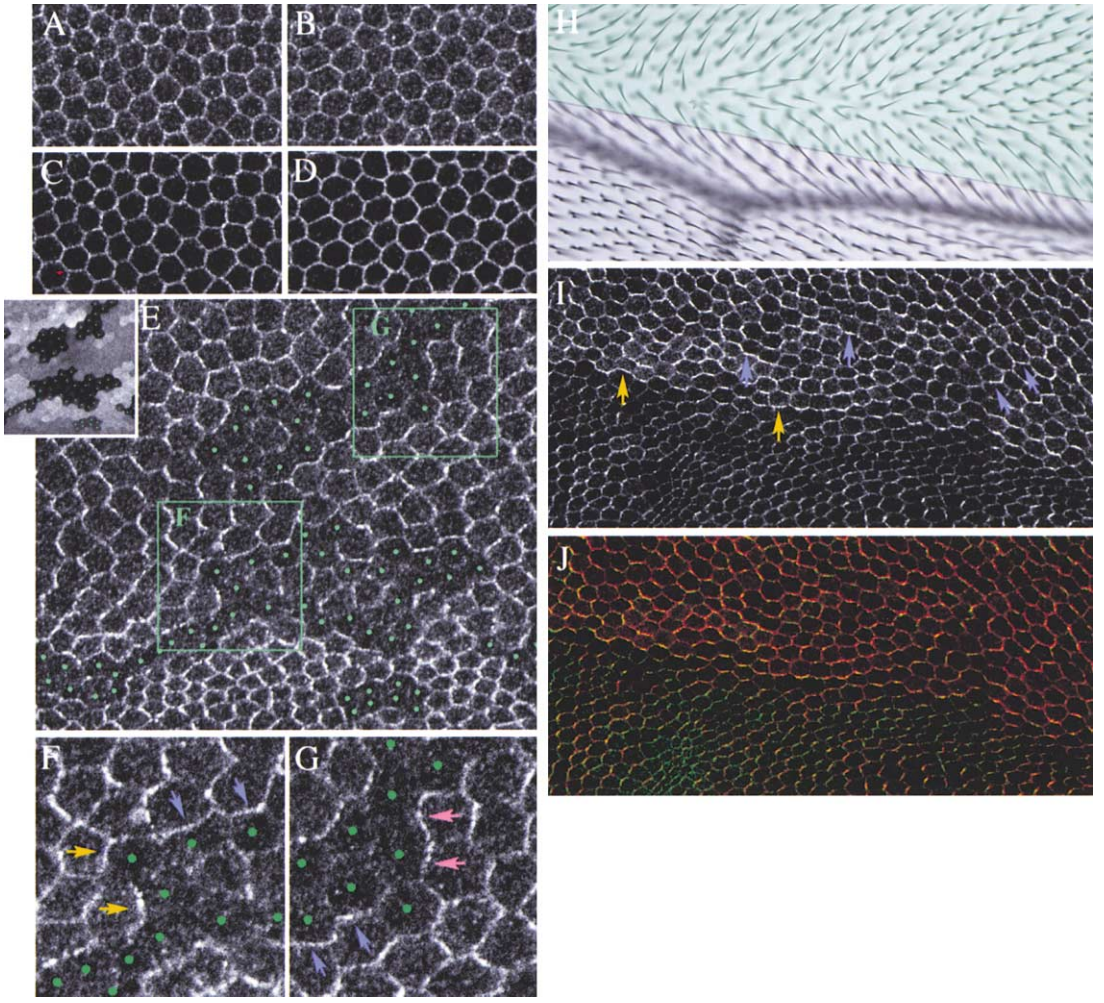

Figure 3. Pk Localization in Fz and Dsh Mutant Tissue

Confocal images of pupal wings.

(A and B) Pk protein is symmetrically distributed in fz^{R52} (A) and dsh^{1} (B) 30 hr APF pupal wings.

(C and D) The same wings were simultaneously stained for Fmi.

(E–G) Pk staining in a wing containing fz^{R52} mutant clones. The mutant cells were marked by absence of Ubi-GFP (E′) and are indicated by green dots.

(F and G) High-magnification images of the areas in the green boxes in (E). Pk is present at a reduced level within the clones and accumulates to high levels at the proximal (yellow arrows), distal (pink arrows), anterior and posterior (blue arrows) boundaries of the clones.

(H) Polarity disruption in the region where Fz is overexpressed in *ptc-GAL4/UAS-fz* flies. The approximate location of the Fz overexpression domain is shaded green.

(I) Pk localization in a *ptc-GAL4/UAS-fz* wing. Smaller cells form the vein primordia; similar regions of the wings in (H) and (I) are shown. Near the posterior border of the *ptc-GAL4* domain, where hairs are oriented posteriorly, Pk localizes between cells expressing high and low levels of Fz (yellow arrows) and is perpendicular to the wild-type orientation. Note the reorganization of polarity and Pk localization (blue arrows) seen at a distance from the edge of the overexpression domain.

(J) Pk and Dsh colocalize in *ptc-GAL4/UAS-fz* wings (Pk, red; Dsh:GFP, green).

all the boundaries between wild-type and *fz* mutant cells (Figures 3F and 3G, arrows). In mutant cells immediately inside the border of the clone, Pk preferentially localizes to the clone borders. Further interior to the clone, symmetrically distributed Pk is observed. Even at the anterior and posterior ends of the clones, Pk tends to accumulate at the clone borders (blue arrows) rather than at the P-D boundaries where it is normally seen. Pk localization, therefore, shows a preference for boundaries between cells expressing different levels of Fz.

As an additional test, cells overexpressing Fz were juxtaposed with wild-type cells in a stripe along the P-D axis of the wing (*ptc-GAL4/UAS-fz*), which results in reorganized polarity perpendicular to the normal axis (Figure 3H). Similar to previous reports for Fmi, Diego, and Dsh, Pk protein localizes along the anterior-posterior boundaries of cells near the edge of the Fz overexpression domain, perpendicular to its normal orientation (Figures 3I and 3J; Axelrod, 2001; Feiguin et al., 2001; Usui et al., 1999). We conclude that differences in Fz levels between adjacent cells are responsible for asymmetric localization of Pk; in the wild-type, high levels of

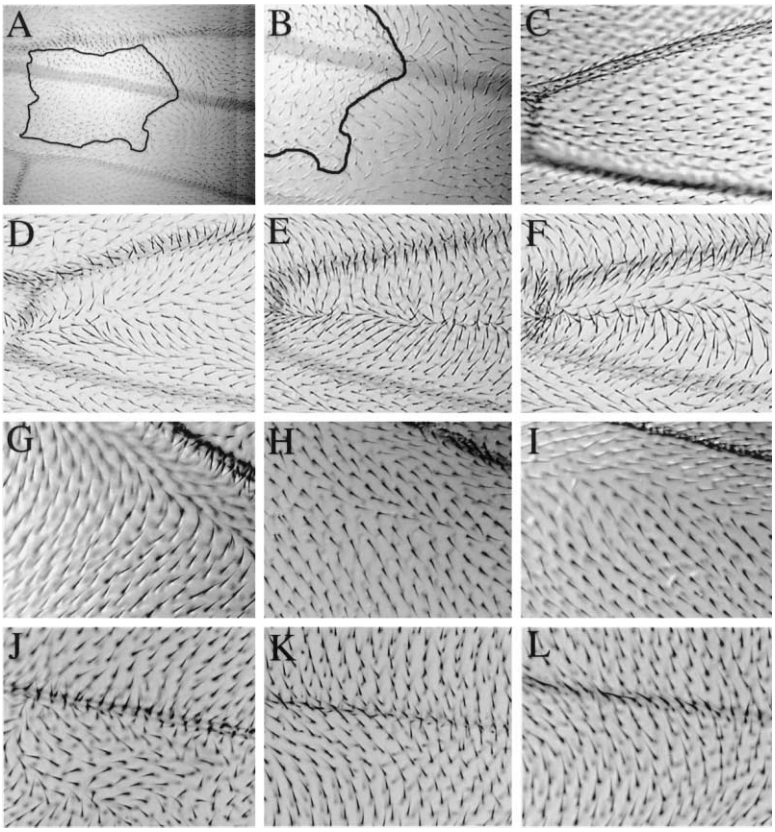

Figure 4. Pk Overexpression and Ordering of Function

(A and B) Dorsal surface of an adult wing bearing a clone overexpressing Pk. The clone is marked with *forked* and outlined in black. (B) A higher magnification of the distal end of the clone shown in (A).

(C–F) Comparison of phenotypes resulting from overexpressing Pk and Fz. Dorsal surfaces of adult wings between L3 and L4, distal to the anterior crossvein. In a wild-type wing, all the wing hairs point distally (C); in *UAS-pk / ptc-Gal4* (E) or *UAS-sple / ptc-Gal4* (F), the wing hairs point toward the midline of the wing, whereas in *UAS-fz / ptc-Gal4* (D), hairs point away from the midline.

(G–L) Ordering the functions of Fz, Dsh, and Pk. Adult wing phenotypes between L4 and L5 and distal to the posterior crossvein produced by *hs-dsh / +* (G), *hs-dsh / +; fz* (H) and *fz* (I). The phenotype caused by overexpressing Dsh (G) is completely suppressed in a *fz* mutant background (H), and the phenotype resembles *fz* (I). Adult wing phenotypes bordering L3, distal to the posterior crossvein, produced by *hs-dsh / +* (J); *pk*; *hs-dsh* (K) and *pk* (L). The phenotype caused by overexpressing Dsh (J) is completely suppressed in a *pk* mutant background (K) with the resulting double mutant resembling *pk* (L).

Fz at the distal side of the cell are therefore proposed to lead to high levels of Pk at the proximal side of the adjacent cell.

Overexpression of Pk and Fz Produce Opposing Effects

A characteristic of the core PCP genes is that their overexpression produces PCP phenotypes that, while qualitatively similar to the loss-of-function phenotypes, display distinct patterns of polarity disruption (Krasnow and Adler, 1994; Axelrod et al., 1998; Gubb et al., 1999; Usui et al., 1999). To further assess the function of Pk, we overexpressed Pk in marked clones in the wing. Overexpression of either the Pk^{Pk} (Figures 4A and 4B) or Pk^{Sple} (not shown) isoforms in clones produces a nonautonomous phenotype, inducing cells distal to the clone to point toward the clone. The phenotype is strikingly similar to that shown by *fz* loss-of-function clones, which also produce a distal domineering nonautonomy, inducing hairs distal to the clone to point toward the clone (Vinson and Adler, 1987).

Because Pk overexpression in clones phenocopies *fz* loss-of-function clones, we infer that they have antagonistic effects on hair polarity. As an additional test of this, we compared the wing hair polarity patterns produced by overexpressing either Fz or Pk (Figures 4C–4F). We used the Gal4/UAS system (Brand and Perrimon, 1993) to drive overexpression of Fz or two isoforms of Pk in a stripe along the antero-posterior boundary. As previously shown, Fz overexpression causes wing hairs to point away from the center of the expression domain, from high toward low levels of Fz (Adler et al., 1997); Figure 4D). In contrast, overexpressing either Pk^{Pk} (Figure 4E) or Pk^{Sple} (Figure 4F) causes wing hairs to point toward the center of the expression domain, pointing from low toward high levels of Pk. Simultaneous overexpression of both Pk^{Pk} and Pk^{Sple} produces a qualitatively similar but stronger phenotype (data not shown). Overexpression of Pk and Fz, therefore, produce opposite effects on wing-hair polarity. Together with the similarity of Pk overexpression clones to loss-of-function *fz* clones, these data imply that Pk and Fz antagonize each other in PCP signaling. Since Pk localizes to the proximal boundary of cells, while Fz is elevated at the distal boundary, this suggests that Pk may facilitate PCP signaling by blocking Fz accumulation at proximal cell boundaries.

Pk Binds Dsh and Blocks Its Cortical Localization

We sought to understand how Pk antagonizes Fz activity by identifying physical interactions between Pk and other PCP signaling components. Using a glutathione-S-transferase (GST) pull-down assay, we found that full-length, in vitro translated Pk^{Sple} bound to a GST-Dsh fusion protein but not to GST alone (Figure 5A). To determine the domain dependency of this interaction, we tested domains of Pk for binding to individual Dsh domains. We found that a Pk construct containing just the conserved PET and LIM domains that are common to all Pk isoforms (PkPETLIM), but not either domain individually, is sufficient for binding to full-length Dsh (not shown). Furthermore, of the three defined Dsh domains,

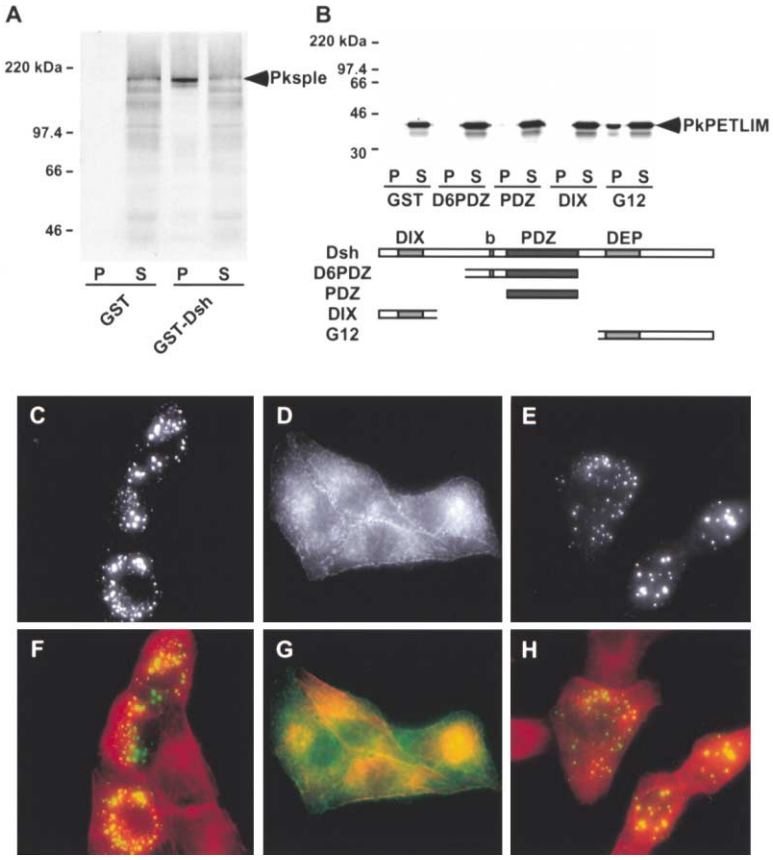

Figure 5. Pk Binds Dsh and Blocks Dsh Membrane Association

(A) Interaction between Pk^{Sple} and Dsh in a GST pull-down assay. [^{35}S]methionine Pk^{Sple}, produced and labeled in vitro, was incubated with bacterially expressed GST and GST-Dsh. [^{35}S]methionine Pk^{Sple} bound GST-Dsh but not GST alone.

(B) Domain analysis of Dsh-Pk binding. [^{35}S]methionine Pk-PETLIM bound Dsh-G13, which contains the DEP domain of Dsh fused to GST, but not the DIX or basic-PDZ domains fused to GST. In (A) and (B), eluted protein from the beads (P) and one-tenth of the supernatant (S) were separated by SDS-PAGE.

(C–E) Dsh::GFP alone.

(C and F) Pk affects Fz-dependent membrane localization of Dsh in U20S cells. Dsh::GFP was transfected into human U20S cells where it was seen in punctae in the cytoplasm.

(D and G) On cotranfection with Fz, Dsh::GFP was translocated to the plasma membrane.

(E and H) Cotranfection of Dsh::GFP, Fz, and Pk consistently resulted in Dsh-GFP localizing to punctae in the cytoplasm. Dsh::GFP appeared to accumulate at lower levels in the Dsh::GFP-, Fz-, and Pk-transfected cells than those transfected with Dsh::GFP alone, though no quantitation was undertaken.

(F–H) Dsh::GFP (green) and phalloidin stained F-actin (red).

DIX, PDZ, and DEP, we found that PkPETLIM bound a construct containing the DEP domain but not other Dsh domains (Figure 5B). The binding between Pk and Dsh was confirmed, and the domain specificity was verified, using a yeast two-hybrid assay. PkPETLIM fused to a DNA binding domain interacted specifically with the Dsh DEP domain but not with the other domains of Dsh (data not shown). We conclude that Pk, via its conserved PET and LIM domains, binds the Dsh DEP domain.

Since the Dsh DEP domain is required for membrane localization, we hypothesized that Pk antagonizes Fz activity by interfering with Dsh membrane localization. To test this, it was necessary to find conditions in which Pk activity was uncoupled from Fz/Dsh activity in the adjacent cell. We therefore reconstituted Fz-dependent Dsh localization in cultured cells. In U20S cells, transfected GFP-tagged Dsh (Dsh::GFP) can be seen in punctate patches in the cytoplasm (Figures 5C and 5F). On cotransfection with Fz, Dsh::GFP is translocated to the cell membrane, as was seen in a similar frog animal cap assay (Figures 5D and 5G; Axelrod et al., 1998). To test whether the physical interaction between Pk and Dsh affects Dsh membrane localization, we cotransfected Fz, Dsh::GFP, and Pk. Dsh is localized in the cytoplasm in 90% of the cotransfected cells, resembling cells transfected with Dsh::GFP alone (Figures 5E and 5H). In contrast, Pk lacking the PET domain is severely impaired in its ability to block Dsh membrane localization (not shown). Pk, therefore, interferes with Dsh membrane association in this heterologous system and by extension may interfere with Dsh membrane localization at the proximal boundary of pupal wing cells. Since Dsh is required to generate asymmetric localization of Fz (Strutt, 2001), we suggest that blocking Dsh membrane localization also inhibits the accumulation of Fz at the proximal boundary.

Ordering the Functions of Pk, Fz, and Dsh

We have shown that Fz activity on the distal side of the cell is linked to the accumulation of Pk on the proximal side of the adjacent cell and that accumulation of Pk suppresses Fz/Dsh localization at the proximal cell cortex. In this way, Fz and Pk appear to function in a feedback loop rather than a linear signaling pathway. We sought to further understand the ordering of these members of the PCP pathway through epistasis analysis.

The loss-of-function phenotypes of *pk$^{pk\text{-}sple}$*, *dsh*, and *fz* are very similar, suggesting that they activate the same signaling mechanism. However, these similarities make classical genetic epistasis tests difficult to interpret. In previous work, Fz overexpression phenotypes have been used to show that Fz signaling requires Dsh (Krasnow et al., 1995). These results were interpreted as implying that the PCP genes form a linear pathway with Dsh acting downstream of Fz. Consistent with this is the finding that Dsh localization requires Fz protein (Axelrod, 2001). In contrast, other observations do not fit this model. For example, localization of Fz requires Dsh, a presumed "downstream" element of the pathway (Strutt, 2001). Fz localization also requires the other presumed downstream elements Pk, Fmi, and Vang/Stbm (Strutt, 2001).

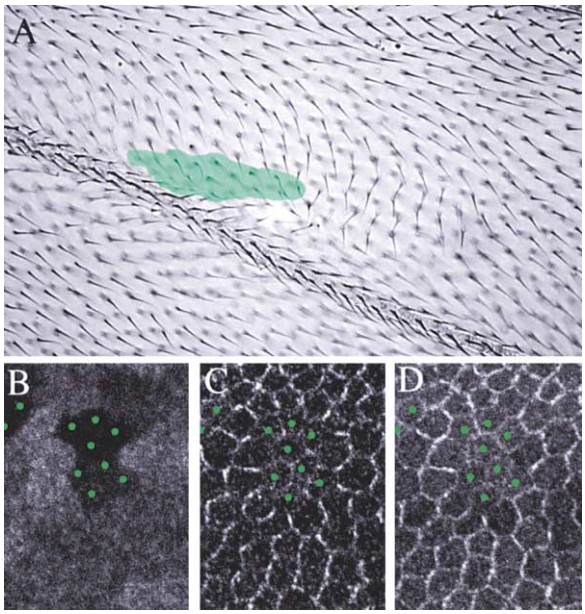

Figure 6. Consequences of Fmi Gain- and Loss-of-Function

(A) An adult wing containing a Fmi overexpression clone, marked with *forked*, in a wild-type background. Mutant cells indicated in green.

(B–D) Confocal images of a 30 hr APF pupal wing containing a fmi^{E59} mutant clone. The mutant cells are indicated with green dots. (B) LacZ marker for fmi^{E59} clone; (C) membrane-associated Pk; and (D) Dsh::GFP proteins within and at the boundaries of the fmi^{E59} clone are at a much reduced level.

To clarify these results, several further epistasis tests were performed. We find that Dsh is required to generate a Fz overexpression phenotype (Krasnow et al., 1995; and data not shown) and that Fz is required to produce a Dsh overexpression phenotype (Figures 4G–4I). In addition, Pk is required for the Dsh (Figures 4J–4L) and Fz (data not shown) overexpression phenotypes. These results argue against a simple linear pathway but are consistent with Fz, Dsh, and Pk participating in a feedback loop.

Evidence that Fmi Acts with Pk on the Proximal Side of the Cell

Like Pk, overexpression of *fmi* using *ptc-Gal4* causes hairs to point toward the midline of the wing (Usui et al., 1999). We also found that *fmi* overexpression clones show distal-domineering nonautonomy, phenocopying *fz* loss-of-function and *pk* overexpression clones (Figure 6A). Thus, it is possible that Fmi could be acting similarly to Pk in feedback amplification of PCP signaling. Fmi is likely to be present at both sides of the cell (Usui et al., 1999), but it may act with Pk at the proximal side to suppress Fz signaling. However, Fmi must have an additional function since, within and surrounding *fmi* clones, very little Pk (Figure 6C) and Dsh (Figure 6D) localize to cell boundaries. In addition to functioning with Pk to suppress Fz/Dsh activity, we suggest that Fmi could have a role in stabilizing the Fz complex at the membrane, without which no signaling occurs.

Pk Overexpression Promotes Assembly of Signaling Complexes

We next tested whether differences in Pk activity between adjacent cells affect the localization of Dsh and Fz. *pk* was overexpressed in the posterior of the wing (using *UAS-pk, engrailed-Gal4*), and Dsh and Fz localization were assessed near the edge of the *pk* overexpression domain. Dsh and Fz were relocalized to the anteroposterior cell boundaries, indicating that accumulation of Dsh and Fz occurs at interfaces between cells expressing high and low levels of Pk (Figures 7A and 7B; arrowheads). Furthermore, within the posterior domain, Dsh and Fz are seen to accumulate to higher levels than in the anterior, consistent with a role for Pk in promoting PCP signaling. We draw two conclusions from these observations. First, Dsh and Fz localization occur preferentially at boundaries between cells expressing high and those expressing lower levels of Pk. Second, providing high levels of Pk amplifies Fz signaling, as measured by the increased accumulation of both Fz and Dsh at cell peripheries. In the wild-type, therefore, Pk at the proximal side of the cell drives Fz and Dsh accumulation at the distal side of the adjacent cell. Conversely, providing high levels of Fz induces higher levels of Pk accumulation (Figure 3I).

Since Pk accumulates at boundaries between cells expressing different levels of Fz, and Dsh accumulates at boundaries between cells expressing different levels of Pk, we suggest that Fz and Dsh on one side and Pk on the opposite side of an intercellular boundary form a self-organizing complex. Indeed, we find evidence for this in the posterior, *pk*-overexpressing domain of the same wings. In the posterior, Dsh and Fz accumulate in discrete patches around the cell peripheries (Figures 7A and 7B). Simultaneous staining for Pk, Dsh, and Fmi, or Fz and Fmi, reveals that all four proteins colocalize to these patches (Figures 7B, 7C, and 7D–7G). Thus, Pk, Dsh, Fmi, and Fz form self-organizing complexes bridging adjacent cells.

Discussion

Various models have been proposed for the distribution of PCP information within *Drosophila* epithelia (Adler, 1992; Eaton, 1997; Gubb, 1998; Shulman et al., 1998; Yang et al., 2002). Regardless of which model is correct, it is likely that this cue induces only a slight asymmetry within each cell. In the *Drosophila* wing, this initial small asymmetry may result in slightly higher levels of Fz accumulation or activation on the distal than on the proximal side of cells. However, this initial level of asymmetry is insufficient to polarize the cytoskeletal architecture of the cell and is undetectable as assessed by Dsh localization (Axelrod, 2001). Fz and Dsh localization subsequently become highly polarized through the action of a feedback amplification loop (Strutt, 2001; Axelrod, 2001). Although the mechanism for such a feedback loop has not been demonstrated, it has previously been speculated that Fz activity on distal cell surfaces might promote expression of an inhibitory Wnt molecule that would suppress Fz activity on the adjacent cell surface (Adler et al., 1997; Taylor et al., 1998). Here, we demonstrate suppression of Fz activity on adjacent cell sur-

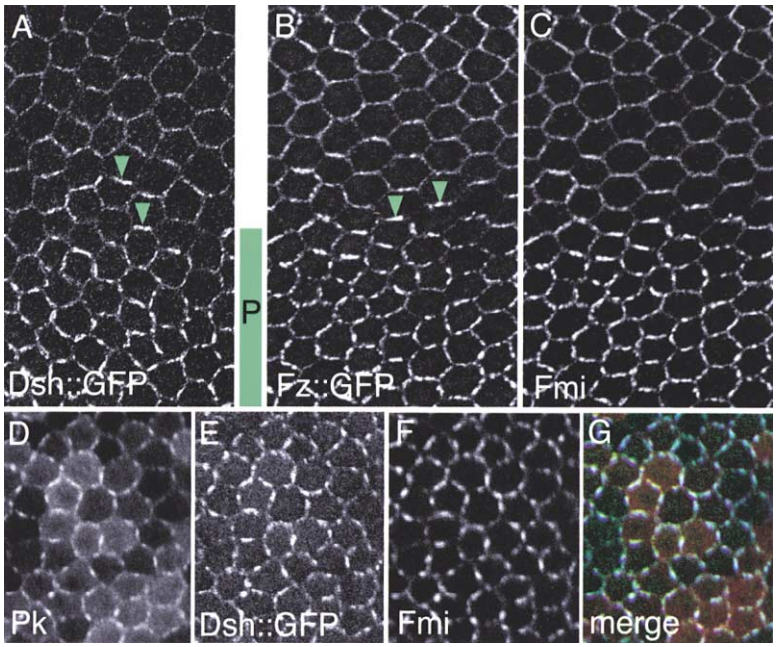

Figure 7. Overexpression of Pk Promotes Assembly of Self-Organizing Complexes

Confocal sections of pupal wings, proximal to the left, anterior up.

(A) Dsh::GFP and (B) Fz::GFP near the anterior-posterior boundary of 30 hr APF pupal wings overexpressing Pk in the *engrailed* domain. Posterior is denoted by the green bar.

(C) The same wing as in (B) stained for Fmi; note that Fz and Fmi colocalize.

(D–G) A region within the posterior compartment of a 30 hr APF pupal wing overexpressing Pk using in the *engrailed* domain, stained for (D) Pk, (E) Dsh::GFP, (F) Fmi, and (G) overlay of Pk (red), Dsh::GFP (green), and Fmi (blue).

faces but find that it is mediated through asymmetric localization of Pk, which antagonizes Fz/Dsh accumulation by blocking cortical Dsh localization.

We propose a model for a Pk-dependent feedback mechanism that functions across each P-D cell interface to amplify the difference between the initial levels of Fz/Dsh activity (Figure 8). Pk and Dsh are initially distributed nearly symmetrically, but in largely nonoverlapping distributions around the cells' apices. As a result of an initial, slight asymmetry in one or more components, Pk suppresses Fz accumulation on the proximal side of the cell by antagonizing Dsh cortical localization. Dsh association with the cortex is required for asymmetric Fz accumulation (Strutt, 2001). Reduced proximal Fz accumulation then decreases Pk activity on the adjacent, distal side of the neighboring cell, allowing even greater Dsh cortical localization and Fz accumulation. Conversely, Pk localization is induced by Fz localization on the neighboring cell. The result is the highly asymmetric distribution of Fz, Dsh, and Pk observed at 30 hr APF. This mechanism is bidirectional, constituting a negative feedback loop that is predicted to be unstable; once any asymmetry is initiated, high levels of Fz/Dsh are promoted on one side of the boundary and low levels on the other. Fmi is proposed to play two roles. The localization of all components to the apical cell cortex depends on Fmi, which is thought to be on both sides of the boundary. Since Fmi overexpression mimics Pk overexpression, we propose that Fmi is activated selectively on the proximal side of the cell, where it works with Pk to suppress Fz/Dsh activity.

In essence, the function of this regulatory loop depends on the balance of forces regulating Dsh membrane association on either side of the boundary. Fz recruits Dsh to the cell cortex, and Pk blocks this recruitment. Once an initial asymmetry is induced, these forces become different on either side of the boundary, and the feedback mechanism amplifies the differences.

Because *fmi* overexpression produces polarity phenotypes very similar to those seen with *pk* overexpression, it is likely that Fmi activity is also polarized across cell boundaries and participates in blocking Fz/Dsh accumulation on the distal side of the interface. However, Fmi has been proposed to exist on both sides of the boundary, and Fmi is required for the efficient localization of Fz, Dsh, and Pk to boundaries. Fmi, therefore, appears to have an additional, complex-stabilizing function. Feiguin et al. (2001) report that Diego (Dgo), an ankyrin repeat protein, is required for PCP signaling and localizes to P-D cell boundaries, though they could not resolve on which side of the boundary it is found. They suggest that Dgo may function as a scaffold for assembly of PCP-signaling components.

The core PCP protein Van Gogh (Vang; Taylor et al., 1998; also known as Strabismus [Stbm]; Wolff and Rubin, 1998), a transmembrane protein, is likely to be involved in the feedback amplification mechanism. In a *vang/stbm* mutant background, Fz is localized symmetrically to the membrane in the same manner as in a *pk* null background (Strutt, 2001), and *vang/stbm* has been proposed to function downstream of *pk* (Taylor et al., 1998). Interestingly, in *Xenopus* and zebrafish, Stbm binds Dsh and seems to toggle its activity between the canonical Wnt and a PCP-like signaling pathway (Park and Moon, 2002). Stbm antagonizes canonical Wnt signaling and activates a PCP-like pathway that regulates convergent extension and induces JNK signaling. We propose that both fly and vertebrate Vang/Stbm may function together with Pk, facilitating PCP signaling by antagonizing Dsh activity.

The feedback amplification mechanism described here provides a clue to understanding the long-standing problem of domineering nonautonomy. Loss-of-function clones of *fz*, *vang/stbm*, and to a lesser extent *pk* induce polarity phenotypes in neighboring wild-type tissue (Vinson and Adler, 1987; Taylor et al., 1998; Gubb

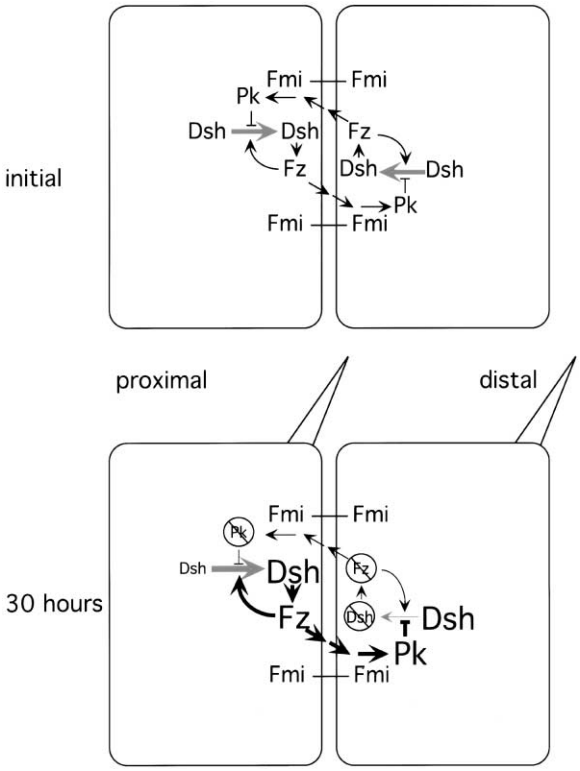

Figure 8. A Model for Feedback Amplification of PCP Signaling

Large bold letters indicate proteins accumulating to high levles; smaller letters indicate lower levels. Bold arrows represent predominant reactions. Circles with slashes indicate proteins whose levels are decreased or absent from the designated locations. Multiple arrows between Fz and Pk indicate that Fz induces accumulation of Pk on the opposite boundary through an undefined mechanism. The initial condition, seen in the early pupal stage, is a nearly symmetric distribution of components in an unstable configuration (initial). A slight imbalance is then imposed on the system by the action of a global cue, biasing the direction of the loop's activity. The relative imbalance of controls on Dsh membrane localization then leads to an amplification of the initial asymmetry, resulting in nearly all the Fz and membrane-associated Dsh accumulating on the distal boundaries, and nearly all the Pk accumulating on the proximal boundaries (30 hr).

et al., 1999). The feedback loop model predicts that loss of Fz will disrupt the localization of these components in the neighboring distal cells, causing their polarity to reverse. Furthermore, if the immediate clone neighbors have reversed polarity, this could then cause the reversal to propagate over a distance. This phenomenon is observed near the lateral borders of a *fz* clone, where Pk accumulation is seen to run parallel to the clone, even at a distance from the mutant cells (Figure 3E). Thus, the reversal in Pk localization may underlie, in part, the domineering nonauontomy observed within wild-type tissue distal to *fz* clones.

Once asymmetrically localized, the Fz/Dsh complex must direct reorganization of the cytoskeleton by both determining the location for prehair initiation and by limiting the number of prehairs to one. Rho and Rho-associated kinase directly regulate myosins to limit the number of prehairs (Winter et al., 2001). The recently described Formin homology protein, Daam1, links Dsh to Rho during vertebrate PCP-like signaling (Habas et al., 2001), and a *Drosophila* homolog may function similarly. However, further studies will be required to understand how localized Fz and Dsh orient prehair initiation.

The feedback loop described here has obvious similarities to lateral signaling by Notch (N) and its ligands Delta (Dl) and Serrate (Ser) (Artavanis-Tsakonas et al., 1999). During lateral signaling, ligand production leads to activation of N on the neighboring cell, which in turn suppresses production of ligand. Thus, an initial imbalance of N or ligand activity is amplified through a feedback loop. One example of lateral signaling by N/Dl is specification of the R3/R4 cell fate decision required to determine PCP in the ommatidia of the *Drosophila* eye (Cooper and Bray, 1999; Fanto and Mlodzik, 1999). Dl production is increased in the R3 neural precursor by high levels of Fz signaling. This leads to increased N activation in R4 and then to the specification of the R4 cell fate needed to produce ommatidial chirality and rotation. Therefore, N/Dl signaling between R3 and R4 is regulated by Fz signaling. However no cell fate decisions appear to be made during PCP specification in the wing, and the N/Dl pathway seems not to be involved in PCP specification in the wing.

Recent evidence implies that elevated Fz activity in R3 compared to R4 is mediated by the same feedback loop described here (Yang et al., 2002). Therefore, two similar mechanisms are used to determine the R3/R4 cell fate decision. First, Fz asymmetry is amplified, and then N asymmetry is amplified. Two steps may be required to execute this decision with high fidelity, or the N pathway may be activated to carry out a cell fate decision in the eye, whereas no such decision is made during PCP signaling in the wing.

The PCP pathway has been implicated in the specification of cell polarity in vertebrate cochlear hair cells and in cell movements in convergent extension (reviewed in Eaton, 1997; Axelrod and McNeill, 2002). It will be of interest to determine how universal this mechanism is in determining epithelial PCP.

Experimental Procedures

Genetics

Mutant genotypes were: (1) *pk$^{pk\text{-}sple13}$ / pk$^{pk\text{-}sple13}$; Dsh::GFP^{III} / +*; (2) *fz^{R52} / fz^{R52}*; (3) *dsh^{1} / Y*; and (4) *ptc-GAL4 / UAS-fz; Dsh::GFP^{III} / +*.

Clones of mutant cells were made using the *FLP/FRT* system (Xu and Rubin, 1993) and marked in pupal wings with *armadillo-lacZ* (Vincent et al., 1994) or *Ubi-GFP* (Davis et al., 1995). Genotypes were: (1) *hs-FLP / + ; FRT 42D pk$^{pk\text{-}sple13}$ / FRT42D armadillo-lacZ; Dsh::GFP^{III} / +*; (2) *hs-FLP / + ; FRT42D fmi^{E59} / FRT42D armadillo-lacZ ; Dsh::GFP^{III} / +*; and (3) *hs-FLP / + ; fz^{R52} FRT2A / Ubi-GFP FRT2A*.

Clones were induced by 2 hr heat shocks during the third instar. White prepupae were then collected and aged at 25°C.

Other lines used were *UAS-fz* (Krasnow and Adler, 1994), *UAS-pk^{pk}*, *UAS-pk^{sple}* (Gubb et al., 1999), *hs-dsh* (Axelrod et al., 1996), *UAS-fmi* (Usui et al., 1999), *Dsh::GFP* (Axelrod, 2001), and *arm-Fz::GFP* (Strutt, 2001). *en-Gal4*, *ptc-Gal4*, and *dpp-Gal4* were obtained from Bloomington stock center. *forked* clones expressing Gal-4 were generated by crossing *hsFLP f^{36}; FRT42D Ubx-FRT<f^{+}>Gal4* (de Celis and Bray, 1997) to *UAS-fmi*, *UAS-pk^{pk}*, or *UAS-pk^{sple}*. Four days after egg laying, progeny were heat shocked for 7 min at 37°C; adult males were examined. Alleles on the second and third chromosomes were balanced over the compound chromosome *SM5a-TM6b*. In subsequent crosses the correct genotypes were identified as non-*Tubby* white prepupae.

Antibodies, Immunostaining, and Microscopy

Rabbit antiserum was raised to a C-terminal fragment of Pk (amino acids 844–1116 of Pk) expressed as a His and thiorodoxin fusion protein in *E. coli* and preabsorbed with His-thiorodoxin bacterial protein extract and with $pk^{pk\text{-}sple13}$ imaginal disc tissue. It was then used at 1:2000. The specificity of the antiserum was demonstrated by absence of staining in the null mutants $pk^{pk\text{-}sple13}$ and $pk^{pk\text{-}sple14}$ (not shown) and in $pk^{pk\text{-}sple13}$ pupal wing clones (Figure 2H). Other antibodies used were mouse anti-LacZ (Promega) and mouse anti-Flamingo (Usui et al., 1999). Pupal wings were stained as described (Axelrod, 2001) and viewed with a laser scanning confocal microscope (Nikon). Adult wings were mounted in Euparal (ASCO Laboratories) and viewed using brightfield microscopy.

Pixel Luminosity

Individual cell boundaries were traced with a standard width line, and the average pixel luminosity, on a scale of 0–255, in the traced region was calculated by Adobe Photoshop. Means and standard deviations for proximal and distal clone boundaries, wild-type and clone interior boundaries were calculated. Assuming normality, a one-tailed Student's t test was used to test significance; we found that the mean for the distal clone boundary is different from the mean for the interior of the clone at a significance value of $p = 0.01$, and proximal is different from wild-type at a value of $p = 0.0002$.

Tissue Culture

U2OS, a human osteosarcoma cell line, was cultured in McCoy's 5A medium supplemented with 10% FBS, 100 U/ml penicillin, 100 μg/ml streptomycin, and 2 mM L-glutamine and incubated at 37°C in 10% CO2. Transfection of constructs was performed with Fugene 6 (Boehringer-Mannheim). Cells (10^5) were plated the day before transfection on 12 mm coverslips treated with fibronectin. Fz and Dsh constructs in pCS2 were as described in Axelrod et al. (1998). Similarly, Pk cDNAs (Gubb et al., 1999) were subcloned into pCS2. In Pk lacking the PET domain, amino acids 442–574 were removed.

GST Pull-Down and Yeast Two-hybrid Assays

Dsh-GST constructs were as described in Rousset et al. (2001) except for G12, which contained Dsh amino acids 394–623 (Willert et al., 1997). Pk^{Sple} full-length cDNA and Pk-PETLIM (Pk^{Sple} amino acids 516–809) were subcloned into pBluescript. GST pull-downs were performed as described in Rousset et al. (2001) except that the final wash contained 80 mM KCl. For yeast two-hybrid experiments, Pk^{Sple} full-length cDNA and Pk-PETLIM were subcloned into pGBKT7 (Promega). All Dsh constructs used were as described in Rousset et al. (2001).

Acknowledgments

We thank Simon Collier, Jose de Celis, Helen McNeill, Mike Simon, and Rebecca Yang for discussions and comments on the manuscript. Thanks to P. Adler, J. Duffy, T. Uemura, and the Bloomington stock center for fly stocks, to K. Willert for GST-Dsh-G12 and -DIX constructs, and to B. and R. Kaiser for help with tissue culture. This work was supported by Medical Research Council program grants (D.G.), by Howard Hughes Medical Institute (R.R. and M.P.S.), and by DRS-16 of the Cancer Research Fund of the Damon Runyon-Walter Winchell Foundation, HHMI, and National Institutes of Health (J.D.A.).

Received: August 14, 2001
Revised: March 7, 2002

References

Adler, P.N. (1992). The genetic control of tissue polarity in *Drosophila*. Bioessays *14*, 735–741.

Adler, P.N., Charlton, J., Jones, K.H., and Liu, J. (1994a). The cold-sensitive period for frizzled in the development of wing hair polarity ends prior to the start of hair morphogenesis. Mech. Dev. *46*, 101–107.

Adler, P.N., Charlton, J., and Park, W.J. (1994b). The *Drosophila* tissue polarity gene inturned functions prior to wing hair morphogenesis in the regulation of hair polarity and number. Genetics *137*, 829–836.

Adler, P.N., Krasnow, R.E., and Liu, J. (1997). Tissue polarity points from cells that have higher Frizzled levels towards cells that have lower Frizzled levels. Curr. Biol. *7*, 940–949.

Artavanis-Tsakonas, S., Rand, M.D., and Lake, R.J. (1999). Notch signaling: cell fate control and signal integration in development. Science *284*, 770–776.

Axelrod, J.D. (2001). Unipolar membrane association of Dishevelled mediates Frizzled planar cell polarity signaling. Genes Dev. *15*, 1182–1187.

Axelrod, J.D., and McNeill, H. (2002). Coupling planar cell polarity signaling to morphogenesis. TheScientificWorld (in press) http://www.thescientificworld.com.

Axelrod, J.D., Matsuno, K., Artavanis-Tsakonas, S., and Perrimon, N. (1996). Dishevelled mediates interaction between Wingless and Notch signaling pathways. Science *271*, 1826–1832.

Axelrod, J.D., Miller, J.R., Shulman, J.M., Moon, R.T., and Perrimon, N. (1998). Differential recruitment of Dishevelled provides signaling specificity in the Planar Cell Polarity and Wingless signaling pathways. Genes Dev. *12*, 2610–2622.

Bhanot, P., Brink, M., Harryman Samos, C., Hsieh, J.-C., Wang, Y., Macke, J.P., Andrew, D., Nathans, J., and Nusse, R. (1996). A new member of the *frizzled* family from *Drosophila* functions as a Wingless receptor. Nature *382*, 225–230.

Bhanot, P., Fish, M., Jemison, J.A., Nusse, R., Nathans, J., and Cadigan, K.M. (1999). Frizzled and DFrizzled-2 function as redundant receptors for wingless during *Drosophila* embryonic development. Development *126*, 4175–4186.

Bhat, K.M. (1998). frizzled and frizzled 2 play a partially redundant role in wingless signaling and have similar requirements to wingless in neurogenesis. Cell *95*, 1027–1036.

Brand, A., and Perrimon, N. (1993). Targeted gene expression as a means of altering cell fates and generating dominant phenotypes. Development *118*, 401–415.

Chae, J., Kim, M.J., Goo, J.H., Collier, S., Gubb, D., Charlton, J., Adler, P.N., and Park, W.J. (1999). The *Drosophila* tissue polarity gene starry night encodes a member of the protocadherin family. Development *126*, 5421–5429.

Chen, C.M., and Struhl, G. (1999). Wingless transduction by the Frizzled and Frizzled2 proteins of *Drosophila*. Development *126*, 5441–5452.

Cooper, M.T., and Bray, S.J. (1999). Frizzled regulation of Notch signalling polarizes cell fate in the *Drosophila* eye. Nature *397*, 526–530.

Davis, I., Girdham, C.H., and O'Farrell, P.H. (1995). A nuclear GFP that marks nuclei in living *Drosophila* embryos; maternal supply overcomes a delay in the appearance of zygotic fluorescence. Dev. Biol. *170*, 726–729.

de Celis, J.F., and Bray, S. (1997). Feed-back mechanisms affecting Notch activation at the dorsoventral boundary in the *Drosophila* wing. Development *124*, 3241–3251.

Eaton, S. (1997). Planar polarization of *Drosophila* and vertebrate epithelia. Curr. Opin. Cell Biol. *9*, 860–866.

Fanto, M., and Mlodzik, M. (1999). Asymmetric Notch activation specifies photoreceptors R3 and R4 and planar polarity in the *Drosophila* eye. Nature *397*, 523–526.

Feiguin, F., Hannus, M., Mlodzik, M., and Eaton, S. (2001). The Ankyrin repeat protein Diego mediates Frizzled-dependent planar polarization. Dev. Cell *1*, 93–103.

Gubb, D. (1993). Genes controlling cellular polarity in *Drosophila*. Dev. Suppl., 269–277.

Gubb, D. (1998). Cellular polarity, mitotic synchrony and axes of symmetry during growth. Where does the information come from? Int. J. Dev. Biol. *42*, 369–377.

Gubb, D., and Garcia-Bellido, A. (1982). A genetic analysis of the determination of cuticular polarity during development in *Drosophila melanogaster*. J. Embryol. Exp. Morphol. *68*, 37–57.

Gubb, D., Green, C., Huen, D., Coulson, D., Johnson, G., Tree, D., Collier, S., and Roote, J. (1999). The balance between isoforms of the prickle LIM domain protein is critical for planar polarity in *Drosophila* imaginal discs. Genes Dev. *13*, 2315–2327.

Habas, R., Kato, Y., and He, X. (2001). Wnt/Frizzled activation of Rho regulates vertebrate gastrulation and requires a novel Formin Homology protein Daam1. Cell *107*, 843–854.

Klingensmith, J., Nusse, R., and Perrimon, N. (1994). The *Drosophila* segment polarity gene dishevelled encodes a novel protein required for response to the wingless signal. Genes Dev. *8*, 118–130.

Krasnow, R.E., and Adler, P.N. (1994). A single *frizzled* protein has a dual function in tissue polarity. Development *120*, 1883–1893.

Krasnow, R.E., Wong, L.L., and Adler, P.N. (1995). *Dishevelled* is a component of the *frizzled* signaling pathway in *Drosophila*. Development *121*, 4095–4102.

Parent, C.A., Blacklock, B.J., Froehlich, W.M., Murphy, D.B., and Devreotes, P.N. (1998). G protein signaling events are activated at the leading edge of chemotactic cells. Cell *95*, 81–91.

Park, M., and Moon, R.T. (2002). The planar cell polarity gene *strabismus* encodes a Dishevelled-associated protein that regulates cell behavior and cell fate in vertebrate embryos. Nat. Cell Biol. *4*, 20–25.

Reifegerste, R., and Moses, K. (1999). Genetics of epithelial polarity and pattern in the *Drosophila* retina. Bioessays *21*, 275–285.

Servant, G., Weiner, O.D., Herzmark, P., Balla, T., Sedat, J.W., and Bourne, H.R. (2000). Polarization of chemoattractant receptor signaling during neutrophil chemotaxis. Science *287*, 1037–1040.

Shulman, J.M., Perrimon, N., and Axelrod, J.D. (1998). Frizzled signaling and the developmental control of cell polarity. Trends Genet. *14*, 452–458.

Strutt, D.I. (2001). Asymmetric localization of Frizzled and the establishment of cell polarity in the *Drosophila* wing. Mol. Cell *7*, 367–375.

Strutt, H., and Strutt, D. (1999). Polarity determination in the *Drosophila* eye. Curr. Opin. Genet. Dev. *9*, 442–446.

Taylor, J., Abramova, N., Charlton, J., and Adler, P.N. (1998). Van gogh. A new drosophila tissue polarity gene. Genetics *150*, 199–210.

Thiesen, H., Purcell, J., Bennett, M., Kansagara, D., Syed, A., and Marsh, J.L. (1994). *dishevelled* is required during *wingless* signaling to establish both cell polarity and cell identity. Development *120*, 347–360.

Usui, T., Shima, Y., Shimada, Y., Hirano, S., Burgess, R.W., Schwarz, T.L., Takeichi, M., and Uemura, T. (1999). Flamingo, a seven-pass transmembrane cadherin, regulates planar cell polarity under the control of Frizzled. Cell *98*, 585–595.

Vincent, J.P., Girdham, C.H., and O'Farrell, P.H. (1994). A cell-autonomous, ubiquitous marker for the analysis of *Drosophila* genetic mosaics. Dev. Biol. *164*, 328–331.

Vinson, C.R., and Adler, P.N. (1987). Directional non-cell autonomy and the transmission of polarity information by the *frizzled* gene of *Drosophila*. Nature *329*, 549–551.

Vinson, C.R., Conover, S., and Adler, P.N. (1989). A *Drosophila* tissue polarity locus encodes a protein containing seven potential transmembrane domains. Nature *338*, 263–264.

Willert, K., Brink, M., Wodarz, A., Varmus, H., and Nusse, R. (1997). Casein kinase 2 associates with and phosphorylates dishevelled. EMBO J. *16*, 3089–3096.

Winter, C.G., Wang, B., Ballew, A., Royou, A., Karess, R., Axelrod, J.D., and Luo, L. (2001). *Drosophila* Rho-associated kinase (Drok) links Frizzled-mediated planar cell polarity signaling to the actin cytoskeleton. Cell *105*, 81–91.

Wolff, T., and Rubin, G.M. (1998). Strabismus, a novel gene that regulates tissue polarity and cell fate decisions in *Drosophila*. Development *125*, 1149–1159.

Wong, L.L., and Adler, P.N. (1993). Tissue polarity genes of *Drosophila* regulate the subcellular location for prehair initiation in pupal wing hairs. J. Cell Biol. *123*, 209–221.

Yang, C.-h., Axelrod, J.D., and Simon, M.A. (2002). Regulation of Frizzled by Fat-like cadherins during planar polarity signaling in the *Drosophila* compound eye. Cell, *108*, 675–688.

Xu, T., and Rubin, G.M. (1993). Analysis of genetic mosaics in developing and adult *Drosophila* tissues. Development *117*, 1223–1237.